Nonlin. Processes Geophys. Discuss., doi:10.5194/npg-2016-61, 2016
Manuscript under review for journal Nonlin. Processes Geophys.
Published: 17 October 2016

Nonlinear Processes in Geophysics
Discussions
Open Access
EGU

OCEAN SWELL WITHIN THE KINETIC EQUATION FOR WATER WAVES

Sergei I. Badulin[1,2] and Vladimir E. Zakharov[1,2,3,4,5]

[1]P. P. Shirshov Institute of Oceanology of the Russian Academy of Science, Russia
[2]Novosibirsk State University, Russia
[3]University of Arizona, Tuscon, USA
[4]P.N. Lebedev Physical Institute of Russian Academy of Sciences
[5]Waves and Solitons LLC, Phoenix, Arizona, USA

Correspondence to: S. I. Badulin (badulin.si@ocean.ru)

Abstract. Results of extensive simulations of swell evolution within the duration-limited setup for the kinetic Hasselmann equation at long times up to 10^6 seconds are presented. Basic solutions of the theory of weak turbulence, the so-called Kolmogorov-Zakharov solutions, are shown to be relevant to the results of the simulations. Features of self-similarity of wave spectra are detailed and their impact on methods of ocean swell monitoring are discussed. Essential drop of wave energy (wave height) due to wave-wave interactions is found to be pronounced at initial stages of swell evolution (of order of 1000 km for typical parameters of the ocean swell). At longer times wave-wave interactions are responsible for a universal angular distribution of wave spectra in a wide range of initial conditions. Weak power-law attenuation of swell within the Hasselmann equation is not consistent with results of ocean swell tracking from satellite altimetry and SAR (Synthetic Aperture Radar) data. At the same time, the relatively fast weakening of wave-wave interactions makes the swell evolution sensitive to other effects. In particular, as shown, coupling with locally generated wind waves can force the swell to grow at rather light winds.

1 Physical models of ocean swell

Ocean swell is an important constituent of the field of surface gravity waves in the sea and, more generally, of the sea environment as a whole. Swell is usually defined as a fraction of wave field that does not depend (or depends slightly) on local wind. Being generated in confined stormy areas these waves can propagate long distances of many thousand miles, thus, influencing vast ocean stretches. For example, swell from Roaring Forties in the Southern Ocean can traverse the Pacifica and reach distant shores of California and Kamchatka. Predicting of swell as a part of sea wave forecast remains a burning problem for maritime safety and marine engineering.

Pioneering works by Munk et al. (1963); Snodgrass et al. (1966) discovered a rich physics of the phenomenon and gave first examples of accurate measurements of magnitudes, periods and directional spreading of swell. Both articles contain thorough discussions of physical background of swell generation, attenuation and interaction with other types of ocean motions. Nonlinear wave-wave interactions have been sketched in these articles as a novelty introduced by the milestone papers by Phillips (1960) and Hasselmann (1962). A possible important role of these interactions at high swell heights for relatively short

Nonlin. Processes Geophys. Discuss., doi:10.5194/npg-2016-61, 2016
Manuscript under review for journal Nonlin. Processes Geophys.
Published: 17 October 2016

Nonlinear Processes in Geophysics
Discussions
Open Access
EGU

time (fetch) of evolution has been outlined and estimated. The first estimates of the observed rates of swell attenuation have been carried out by Snodgrass et al. (1966) based on observation at near-shore stations. Their characteristic scale (e-folding) about 4000 km is consistent with some today results of the satellite tracking of swell (Ardhuin et al., 2009, 2010; Jiang et al., 2016) and with treatment of these results within the model of swell attenuation due to coupling with turbulent atmospheric layer. Alternative model of turbulent wave flow attenuation (Babanin, 2006) predicts quite different algebraic law and stronger swell attenuation at shorter distances from the swell source (Young et al., 2013). It should be stressed that all the mentioned models treat swell as a quasi-monochromatic wave and, thus, ignore nonlinear interactions of the swell harmonics themselves and the swell coupling with locally generated wind-wave background. The latter effect can be essential as observations and simulations clearly show (e.g. Pettersson, 2004; Young, 2006; Badulin et al., 2008b, and refs. therein).

The swell is generally considered as a superposition of harmonics that do not interact to each other and, thus, can be described by the well-known methods of the linear theory of waves (e.g. Snodgrass et al., 1966). Many features of the observed swell can be related to such models. For example, the observed linear growth of the swell frequency in a site can be explained as an effect of dispersion of a linear wave packet over long time. The linear models of swell dissipation lead, evidently, to exponential laws of the swell energy (height) attenuation and to attempts to estimate the e-folding scale from available experimental data (e.g. Snodgrass et al., 1966; Jiang et al., 2016).

Synthetic aperture radars (SAR) allow for spatial resolution up to tens meters and, thus, for detecting relatively long swell of a few hundred meters wavelength along their thousand miles tracks (e.g. Ardhuin et al., 2010; Young et al., 2013). Satellite altimeters measure wave height averaged over a snapshot of a few square kilometers that is adequate to the today methods of statistical description of waves in the research and application models and also can be used for the swell tracking in combination with other tools (e.g. wave models as in Jiang et al., 2016). Re-tracking of swell allows, first, for relating the swell events with their probable sources – stormy areas. Secondly, the swell transformation gives a clue to estimating effects of other motions of the ocean (e.g. Chen et al., 2002). Such work requires adequate physical models of swell propagation and transformation as far as a number of parameters of sea environment remains beyond control.

Meanwhile, the linear treatment remains quite restrictive and cannot explain important features of swell. First, the observed swell spectra exhibit frequency downshift which is not predicted by deterministic linear or weakly nonlinear models of narrow-banded wave guide evolution (e.g. data of Snodgrass et al., 1966, and comments on these data by Henderson and Segur (2013)). Secondly, these spectra show invariance of their shapes that is unlikely to be appear in linear dispersive wave system. All the noted features are common for wave spectra described by the kinetic equation for water waves, the so-called Hasselmann (1962) equation.

In this paper we present results of extensive simulations of ocean swell within the Hasselmann equation. The simplest duration-limited setup has been chosen to obtain numerical solutions for the duration up to 10^6 seconds (11.5 days) for typical parameters of ocean swell (wavelengths $150 - 400$ meters, initial significant heights $3 - 10$ meters).

We analyze the simulation results from the viewpoint of the theory of weak turbulence (Zakharov et al., 1992). The slowly evolving swell solutions appear to be quite close to the stationary milestone Kolmogorov-Zakharov solutions for water waves (Zakharov and Filonenko, 1966; Zakharov and Zaslavsky, 1982) in a frequency range and give estimates for the fundamental

Nonlin. Processes Geophys. Discuss., doi:10.5194/npg-2016-61, 2016
Manuscript under review for journal Nonlin. Processes Geophys.
Published: 17 October 2016

Nonlinear Processes in Geophysics
Discussions
Open Access
EGU

constants of the theory. We give a short theoretical introduction and present these estimates in the next section. In sect.3 we relate results of simulations with properties of the self-similar solutions of the kinetic equation. Zaslavskii (2000) was the first who presented the self-similar solutions for swell assuming the angular narrowness of the swell spectra and gave a set of explicit analytical results. In fact, more general consideration in the spirit of Badulin et al. (2002, 2005) leads to important findings and to a number of questions with no reliance upon the assumption of angular narrowness.

We demonstrate the well-known fact that is usually ignored: the power-law swell attenuation within the conservative kinetic equation. We show that it does not contradict to results of observations mentioned above. We also reveal a remarkable feature of collapsing the swell spectra to an angular distribution that depends weakly on initial angular spreading. Such universality can be of great value for modelling swell and developing methods of its monitoring.

The paper is finalized by looking for a niche for the model under discussion. Evidently, the setup of duration-limited evolution is quite restrictive and does not reflect essential features of ocean swell transformation where wave dispersion and spatial divergence play a key role. Meanwhile, significance of some effects remains of importance irrespectively to the setup. In particular, fast weakening of wave-wave interactions in presence of a background of wind-driven waves can switch effectively the swell attenuation to swell amplification. Estimates presented in this paper show possibility of this effect and can help in interpretation of peculiarities of recent observations of swell from space ('negative' dissipation in words of Jiang et al., 2016). Thus, a number of problems of adequate physical description of ocean swell are waiting for their solution. This paper is an attempt to consider some of these problems and to reveal essential features of swell evolution within the simple model of the kinetic Hasselmann equation.

2 Solutions for ocean swell

2.1 The Kolmogorov-Zakharov solutions

In this section we reproduce previously reported theoretical results on evolution of swell as a random field of weakly interacting wave harmonics. We follow the statistical theory of wind-driven seas (Zakharov, 1999) extending this approach to the sea swell which description within this approach is usually considered as questionable. A random wave field is described by the kinetic equation derived by Klauss Hasselmann in early sixties (Hasselmann, 1962) for deep water waves in absence of dissipation and external forcing

$$\frac{\partial N_{\mathbf{k}}}{\partial t} + \nabla_{\mathbf{k}}\omega_{\mathbf{k}}\nabla_{\mathbf{r}}N_{\mathbf{k}} = S_{nl}. \qquad (1)$$

Equation (1) is written for the spectral density of wave action $N(\mathbf{k},\mathbf{x},t) = E(\mathbf{k},\mathbf{x},t)/\omega(\mathbf{k})$ ($E(\mathbf{k},\mathbf{x},t)$ is wave energy spectrum and wave frequency obeys linear dispersion relation $\omega = \sqrt{g|\mathbf{k}|}$). Subscripts for ∇ corresponds to the two-dimensional gradient operator in the corresponding space of coordinates $\mathbf{x}$ and wavevectors $\mathbf{k}$ (i.e. $\nabla_{\mathbf{r}} = (\partial/\partial x, \partial/\partial y)$).

The right-hand term S_{nl} describes the effect of wave-wave resonant interactions and can be written in explicit form (see Appendices in Badulin et al., 2005, for collection of formulas). The cumbersome term S_{nl} causes a number of problems for

Nonlin. Processes Geophys. Discuss., doi:10.5194/npg-2016-61, 2016
Manuscript under review for journal Nonlin. Processes Geophys.
Published: 17 October 2016

Nonlinear Processes in Geophysics
Discussions
Open Access
EGU

wave modelling where (1) is extensively used. Nevertheless, for deep water case one has a key property of the term homogeneity

$$S_{nl}[\kappa\mathbf{k}, \nu N_{\mathbf{k}}] = \kappa^{19/2}\nu^3 S_{nl}[\mathbf{k}, N_{\mathbf{k}}]. \tag{2}$$

that helps in getting important analytical results. Stretching in κ times in wave scale or in ν times in wave action (κ, ν are positive) leads to simple re-scaling of the collision term S_{nl}. This important property gives a clue for constructing power-law stationary solutions of the kinetic equation, i.e. solutions for the equation

$$S_{nl} = 0. \tag{3}$$

Two isotropic stationary solutions of (3) correspond to constant fluxes of wave energy and action in wave scales. The direct cascade solution (Zakharov and Filonenko, 1966) in terms of frequency spectrum of energy

$$E^{(1)}(\omega, \theta) = 2C_p \frac{P^{1/3} g^{4/3}}{\omega^4} \tag{4}$$

introduces the basic Kolmogorov constant C_p and describes the energy transfer to infinitely short waves with constant flux P. The wave action transfer to opposite direction of long waves is described by the inverse cascade solution (Zakharov and Zaslavsky, 1982)

$$E^{(2)}(\omega, \theta) = 2C_q \frac{Q^{1/3} g^{4/3}}{\omega^{11/3}} \tag{5}$$

with wave action flux Q and another Kolmogorov's constant C_q.

An approximate weakly anisotropic Kolmogorov-Zakharov solution has been obtained by Katz and Kontorovich (1974) as an extension of (4)

$$E^{(3)}(\omega, \theta) = 2\frac{P^{1/3} g^{4/3}}{\omega^4}\left(C_p + C_m \frac{gM}{\omega P}\cos\theta + \ldots\right). \tag{6}$$

It associates the wave spectrum anisotropy with the constant spectral flux of wave momentum M and the so-called second Kolmogorov constant C_m. As it is seen from (6) the solution anisotropy vanishes as $\omega \to \infty$: wave spectra become isotropic for short waves. The whole set of the KZ solutions (4–6) can be treated naturally within the dimensional approach: these are just particular cases of solutions of the form

$$E^{(KZ)}(\omega) = \frac{P^{1/3} g^{4/3}}{\omega^4} G(\omega Q/P, gM/(\omega P), \theta) \tag{7}$$

where G is a function of dimensionless arguments scaled by spectral fluxes of energy P, wave action Q and wave momentum M.

Originally, solutions (4–6) have been derived in quite sophisticated and cumbersome ways. Later on, simpler and more physically transparent approaches have been presented (Zakharov and Pushkarev, 1999; Balk, 2000; Pushkarev et al., 2003, 2004; Badulin et al., 2005; Zakharov, 2010). These more general approaches allow for looking at higher-order terms of the anisotropic Kolmogorov-Zakharov solutions (6). In particular, they predict the next term proportional to $\cos 2\theta/\omega^2$ that is the second angular harmonics of the stationary solution.

Nonlin. Processes Geophys. Discuss., doi:10.5194/npg-2016-61, 2016
Manuscript under review for journal Nonlin. Processes Geophys.
Published: 17 October 2016

Swell solutions evolve slowly with time and, thus, give a good opportunity for discussing features of the KZ solutions (or, alternatively, the KZ solutions can be used as a benchmark for the swell studies). One of the key points of this discussion is the question of uniqueness, that can be treated in the context of general KZ solutions (7). While the principal terms of the general Kolomogorov-Zakharov solution corresponding to (4–6) have clear physical meaning of total fluxes of wave action (5), energy (4) and momentum (6) this is not the case of the higher-order terms. The link of these additional terms with inherent properties of the collision integral S_{nl} or/and with specific initial conditions is not a trivial point. In this paper we give the very preliminary answer to this intriguing question.

2.2 Self-similar solutions of the kinetic equation

The homogeneity property (2) is extremely useful for studies of non-stationary (inhomogeneous) solutions of the kinetic equation. Approximate self-similar solutions for reference cases of duration- and fetch-limited development of wave field can be obtained under assumption of dominance of the wave-wave interaction term S_{nl} (Pushkarev et al., 2003; Zakharov, 2005; Badulin et al., 2005; Zakharov and Badulin, 2011). These solutions have forms of the so-called incomplete or the second type self-similarity (e.g. Barrenblatt, 1979). In terms of frequency-angle dependencies of wave action spectra one has for the duration- and fetch-limited cases correspondingly (Badulin et al., 2005, 2007; Zakharov et al., 2015)

$$N(\omega,\theta,\tau) = a_\tau \tau^{p_\tau} \Phi_{p_\tau}(\xi,\theta) \quad (8)$$

$$N(\omega,\theta,\chi) = a_\chi \chi^{p_\chi} \Phi_{p_\chi}(\zeta,\theta) \quad (9)$$

with dimensionless time τ and fetch χ

$$\tau = t/t_0; \qquad \chi = x/x_0. \quad (10)$$

Homogeneity properties (2) dictates ‘magic relations’ (in words of Pushkarev and Zakharov, 2015, 2016) between dimensionless exponents p_τ, q_τ and p_χ, q_χ

$$p_\tau = \frac{9q_\tau - 1}{2}; \qquad p_\chi = \frac{10q_\chi - 1}{2}. \quad (11)$$

Dimensionless arguments of shape functions $\Phi_{p_\tau}(\xi)$, $\Phi_{p_\chi}(\zeta)$ in (8,9) contain free scaling parameters b_τ, b_χ

$$\xi = b_\tau \omega^2 \tau^{-2q_\tau}; \qquad \zeta = b_\chi \omega^2 \chi^{-2q_\chi}. \quad (12)$$

Additional ‘magic relations’ coming from homogeneity property (2) fix a link between the amplitude scales a_τ, a_χ and the bandwidth scales b_τ, b_χ of the self-similar solutions (8–12)

$$a_\tau = b_\tau^{19/4}; \qquad a_\chi = b_\chi^{5/2}. \quad (13)$$

Thus, ‘magic relations’ (11,13) reduce number of free parameters of the self-similar solutions (8,9) from four (two exponents and two coefficients) to two only: a dimensionless exponent p_τ (p_χ) and an amplitude of the solution a_τ (a_χ).

Nonlin. Processes Geophys. Discuss., doi:10.5194/npg-2016-61, 2016
Manuscript under review for journal Nonlin. Processes Geophys.
Published: 17 October 2016

Nonlinear Processes in Geophysics
Discussions
Open Access
EGU

The shape functions $\Phi_\tau(\xi)$, $\Phi_\chi(\zeta)$ in (8,9) are specified by solutions of a boundary problem for an integro-differential equation in self-similar variable ξ (or ζ for fetch-limited case) and angle θ (see sect. 5.2 Badulin et al., 2005, for details). Simulations (e.g. Badulin et al., 2008a) reveal remarkable features of the shape functions $\Phi_\tau(\xi)$, $\Phi_\chi(\zeta)$. First, numerical solutions generally show relatively narrow angular distributions for $\Phi_{p_\tau}(\xi)$, $\Phi_{p_\chi}(\zeta)$ with a single pronounced maximum near a spectral peak frequency ω_p. It implies that the only one (or very few) of an infinite series of eigenfunctions of the boundary problem for the shape functions $\Phi_{p_\tau}(\xi)$, $\Phi_{p_\chi}(\zeta)$ contributes into wave spectra evolution in a wide range of initial and external forcing conditions. This treatment of the heavily nonlinear boundary problem in terms of a composition of eigenfunctions is possible in this case as demonstrated by Zakharov and Pushkarev (1999). Two-lobe patterns are observed at higher frequencies ($\omega > 2\omega_p$) in some cases as local maxima at oblique directions or as a 'shoulder' in wave frequency spectra. Their appearance is generally discussed as an effect of wind on wave generation (e.g. Bottema and van Vledder, 2008, 2009).

Secondly, an important property of *spectral shape invariance* (terminology of Hasselmann et al., 1976) or *the spectra quasi-universality* (in words of Badulin et al., 2005) is widely discussed both for experimentally observed and simulated wave spectra. This invariance does not suppose a point-by-point coincidence of properly normalized spectral shapes. Proximity of integrals of the shape functions Φ_{p_τ}, Φ_{p_χ} in a range of wave growth rates p_τ, p_χ appears to be sufficient for formulating a remarkable universal relationship for parameters of self-similar solutions (8,9)

$$\mu^4\nu = \alpha_0^3. \tag{14}$$

Here wave steepness μ is estimated from total wave energy E and spectral peak frequency ω_p

$$\mu = \frac{E^{1/2}\omega_p^2}{g}. \tag{15}$$

The 'number of waves' ν in a spatially homogeneous wind sea (i.e. for duration-limited wave growth) is defined as follows:

$$\nu = \omega_p t. \tag{16}$$

For spatial (fetch-limited) wave growth the coefficient of proportionality C_f in the equivalent expression $\nu = C_f|\mathbf{k}_p|x$ ($\mathbf{k}_p$ being the wavevector of the spectral peak) is close to the ratio between the phase and group velocities $C_{ph}/C_g = 2$. A universal constant $\alpha_0 \approx 0.7$ is a counterpart of the constants C_p, C_q of the stationary Kolmogorov-Zakharov solutions (4,5) and has a similar physical meaning of a ratio between wave energy and the energy spectral flux (in power $1/3$). A remarkable feature of the universal wave growth law (14) is its independence on wind speed. This wind-free paradigm based on intrinsic scaling of wave development is shown to be a useful tool of analysis of wind-wave growth (Zakharov et al., 2015). Below we demonstrate its effectiveness for results of swell simulations.

Nonlin. Processes Geophys. Discuss., doi:10.5194/npg-2016-61, 2016
Manuscript under review for journal Nonlin. Processes Geophys.
Published: 17 October 2016

Nonlinear Processes in Geophysics
Discussions
Open Access
EGU

2.3 Self-similarity of swell solutions

The self-similar solution for swell is just a member of a family of solutions (8,9) with particular values of temporal or spatial rates

$$p_\tau = 1/11; \qquad q_\tau = 1/11 \tag{17}$$

$$p_\chi = 1/12; \qquad q_\chi = 1/12 \tag{18}$$

Exponents (17,18) provide conservation of the total wave action for its evolution in time (duration-limited setup) or in space (fetch-limited)

$$N = \int_0^\infty N(\omega,\theta)d\omega d\theta = \text{const} \tag{19}$$

On the contrary, total energy and wave momentum are only formal constants of motion of the Hasselmann equation and decay with time t or fetch x

$$E \sim t^{-1/11}; \qquad M \sim t^{-2/11} \tag{20}$$

$$E \sim x^{-1/12}; \qquad M \sim x^{-2/12}. \tag{21}$$

The swell decay (20,21) reflects a basic feature of the kinetic equation for water waves: energy and momentum are not conserved (see Zakharov et al., 1992; Pushkarev et al., 2003, and refs. herein). The wave action is the only true integral of the kinetic equation (1).

The swell solution manifests another general feature of evolving wave spectra: the downshifting of the spectral peak frequency (or other characteristic frequency), i.e.

$$\omega_p \sim t^{-1/11}; \qquad \omega_p \sim x^{-1/12}. \tag{22}$$

The universal law of wave evolution (14) is, evidently, valid for the self-similar swell solution as well with a minor difference in the value of the constant α_0. As soon as this constant is expressed in terms of the integrals of the shape functions Φ_τ, Φ_χ and the swell spectrum shape differs essentially from ones of the growing wind seas this constant appears to be less than α_0 of the growing wind seas.

The theoretical background presented above is used below for analysis of results of simulations.

3 Swell simulations

3.1 Simulation setup

Simulations of ocean swell require special care. First of all, calculations for quite long time (up to 10^6 seconds in our case) should be accurate enough in order to capture relatively slow evolution of solutions and, thus, be able to relate results with

Nonlin. Processes Geophys. Discuss., doi:10.5194/npg-2016-61, 2016
Manuscript under review for journal Nonlin. Processes Geophys.
Published: 17 October 2016

Nonlinear Processes in Geophysics
Discussions
Open Access
EGU

the theoretical background presented above. We used the approach of our previous papers (Badulin et al., 2002, 2005, 2007, 2008a).

Duration-limited evolution has been simulated with the code based on WRT algorithm (Webb, 1978; Tracy and Resio, 1982) for different initial conditions (spatial spectra at $t = 0$). Frequency resolution for log-spaced grid has been set to $(\omega_{n+1} - \omega_n)/\omega_n = 1.03128266$. It corresponds to 128 grid point in frequency range $0.02 - 1$ Hz (approximately 1.5 to 3850 meters wave length). Thus, we used very fine frequency resolution in a wide range of wave scales (cf. Benoit and Gagnaire-Renou, 2007; Gagnaire-Renou et al., 2011) to trace rather slow evolution of swell. Standard angular resolution $\Delta\theta = 10^\circ$ has been taken as adequate to goals of our study.

Initial conditions were similar in all series of simulations: wave action spectral density in a box of frequencies and angles was slightly (5% of magnitude) modulated in angles and had low (six orders less) background outside this box:

$$N(\mathbf{k}) = \begin{cases} N_0(1 + 0.05\cos(\theta^2/2)), |\theta| < \Theta/2, \omega_l < \omega < \omega_h \\ 10^{-6}N_0, \qquad \text{otherwise} \end{cases} \tag{23}$$

The modulations have been set in order to stimulate wave-wave interactions since the collision integral S_{nl} vanishes for $N(\mathbf{k}) = \text{const}$. In contrast to wind waves where wind speed is an essential physical parameter that provides a useful physical scale, the swell evolution is determined by initial conditions only, i.e. by N_0 and Θ in the setup (23).

Dissipation was absent in the runs. Free boundary conditions were applied at the high-frequency end of the domain of calculations: generally, short-term oscillations of the spectrum tail do not lead to instability. Calculations with a hyper-dissipation (e.g. Pushkarev et al., 2003) or a diagnostic tail at the high-frequency range of the spectrum (Gagnaire-Renou et al., 2010) do not affect results even quantitatively as compared with our options of simulations.

Totally, more than 30 runs have been carried out for different initial conditions for duration 10^6 seconds. Below we focus on the series of Table 1 where initial wave heights were fixed (within 2%) and angular spreading varied from very narrow $\Theta = 30^\circ$ to almost isotropic $\Theta = 330^\circ$ (23). The frequency range of the initial perturbations was $0.1 - 0.4$Hz.

3.2 Self-similarity features of swell

Evolution of swell spectra with time is shown in fig.1 for the case `sw330` of Table 1. The example shows a strong tendency to self-similar shaping of wave spectra. This remarkable feature has been demonstrated and discussed for swell in previous works (Badulin et al., 2005; Benoit and Gagnaire-Renou, 2007; Gagnaire-Renou et al., 2010) for special parameters that provided relatively fast evolution of rather short and unrealistically high waves. In our simulations we start with the mean wave period about 3 seconds that corresponds to the end of calculations of Badulin et al. (2005, see fig. 8 therein) and moderately high steepness $\mu \approx 0.15$ as defined by (15). The initial step-like spectrum evolves very quickly and keeps a characteristic shape for less than 1 hour. For 269 hours the spectral peak period reaches 11 seconds (the corresponding wavelength $\lambda \approx 186$ meters) and wave steepness becomes $\mu = 0.023$. The final significant wave height $H_s \approx 2.8$ meters is essentially less than its initial value 4.8 meters. All these values can be considered as typical ones for ocean swell.

Nonlin. Processes Geophys. Discuss., doi:10.5194/npg-2016-61, 2016
Manuscript under review for journal Nonlin. Processes Geophys.
Published: 17 October 2016

Dependence of key wave parameters on time is shown in fig. 2 for different runs of the series of Table 1. Power-law dependencies of self-similar solutions (17,18,20-22) are shown by dashed lines. In fig. 2*a,b* total wave energy E and the spectral peak frequency ω_p show good correspondence to power laws of the self-similar solutions (8). By contrast, power-law decay of the $x-$component of wave momentum M_x depends essentially on angular spreading of initial wave spectra. While for narrow spreading (runs `sw030` and `sw050`) there is no visible deviation from the $M_x \sim t^{-2/11}$ law, wide-angle cases clearly show these deviations. The 'almost isotropic' solution for `sw330` is tending quite slowly to the theoretical dependency in terms of wave momentum M_x (21). The duration more than 11 days appears 'too short' for demonstrating this theoretical result: one can see a transitional behavior when wave spectra evolve from the 'almost isotropic' state to an inherent distribution with a pronounced anisotropy.

A simple quantitative estimate of the 'degree of anisotropy' is given in fig.2*d*. Evolution of dimensionless parameter of anisotropy in terms of the approximate Kolmogorov-Zakharov solution (6) by Katz and Kontorovich (1974) is shown for all the cases of Table 1. We introduce parameter of anisotropy A as follows

$$A = \frac{gM}{\omega_p P}. \tag{24}$$

where total energy flux P (energy flux at $\omega \to \infty$) can be estimated from evolution of total energy

$$P = -\frac{dE}{dt}. \tag{25}$$

Similarly, total wave momentum

$$\mathbf{K} = \int \mathbf{k} N(\mathbf{k}) d\mathbf{k} \tag{26}$$

provides an estimate of its flux in x-direction

$$M_x = -\frac{dK_x}{dt}. \tag{27}$$

Spectral peak frequency ω_p has been used for the definition of 'degree of anisotropy' A (24). Different scenarios are seen in fig. 2*d* depending on angular spreading of wave spectra. Nevertheless, a general tendency to a universal behavior at very large times (more than 10^6 seconds) looks quite plausible.

Similar dispersion of different runs (different anisotropy of initial distributions) is seen in fig. 3 when tracing the invariant of the self-similar solutions (14). Again, like in fig.2b, one million seconds of the swell duration are not sufficient to demonstrate validity of relationship (14) in its full. A limit α_0 (14) is very likely reached at larger times. This limit is a bit less (by approximately 10%) than one for growing wind seas $\alpha_0 \approx 0.7$. Again, the 'almost isotropic' solution shows its stronger departure from the rest of the series. The differences are better seen in angular distributions rather than in normalized spectral shapes (fig. 4) when we are trying to check self-similarity features of the solutions in the spirit of Badulin et al. (2005); Benoit and Gagnaire-Renou (2007).

Nonlin. Processes Geophys. Discuss., doi:10.5194/npg-2016-61, 2016
Manuscript under review for journal Nonlin. Processes Geophys.
Published: 17 October 2016

3.3 Angular spreading of swell spectra

Despite of dramatic difference of the runs in integral characteristics of the swell anisotropy (e.g. figures 2*b,d*) the resulting spectral distributions still show clearly pronounced features of universality. This is of importance in the context of remarks in sect.2.2: does the only eigenfunction (or, more prudently, very few eigenmodes) survive in course of the swell evolution?

Normalized sections of spectra at the peak frequency ω_p are shown in fig.5 for the Table 1 runs at the end of simulations at $t = 10^6$ seconds (approx. 11.5 days). 'The almost isotropic' run `sw330` shows relatively high pedestal of about 3% of maximal value while other series have a background less than 0.2%. At the same time, the core of all distributions is quite close to a gaussian shape

$$y_{gauss} = \exp\left(-\frac{\theta^2}{2\sigma^2}\right) \tag{28}$$

with half-width $\sigma = 35^\circ$ (dashed curve in fig.5). Experimentally based spreading functions are represented in fig.5 by two reference curves. For growing wind seas the dependence by Donelan et al. (1985, eq.9.2)

$$y_{1985} = \mathrm{sech}^2(\beta\theta); \quad \beta = 2.28 \tag{29}$$

gives almost twice sharper distribution (dash-dot in fig.5). The angular distribution by Komen et al. (1984) in simulations of fully developed seas (dotted curve in fig.5)

$$y_{1984} = \cos^p(\theta/2); \quad p = 4.66 \tag{30}$$

predicts wider angular spreading as compared with our results. Relatively wide angular distribution in the swell simulations (28) is somewhat in contradiction with conventional vision of swell as extremely narrow in angle. More accurate measurements of angular characteristics of swell can help to resolve this contradiction.

Evolution of angular spreading in time is shown in fig. 6 for 'the almost isotropic' run `sw330` in absolute values. The sharpening of the angular distribution is accompanied by the peak increase of frequency-angle spectrum while the spectrum magnitude (averaged in angle) is slightly decaying with time (cf. fig. 1).

Angular spreading at higher frequency 1.25ω in fig. 7 for the same run `sw330` is evolving in two stages. First, saturation of the high-frequency tail occurs almost isotropically: for 1 hour only the energy at this frequency jumps by 5 orders in magnitude from the initial background level $10^{-6}N_0$ (see eq.23). Further evolution leads to pronounced sharpening of the distribution and its drift to a universal shape (see fig.5).

The frequency 1.25ω is a characteristic one in the Discrete Interaction Approximation (DIA) for the collision integral S_{nl} which is used extensively in research and forecasting models of sea waves (Hasselmann and Hasselmann, 1985). Thus, fig. 7 illustrate possible problems in simulations of wave-wave interactions with the DIA: the numerical scheme should have rather fine distribution for resolving peculiar features of spectral functions. At large time this figure shows formation of side lobes: maxima of spectral densities for oblique counter-propagating harmonics. Such behavior of wave spectra is reported in many papers (e.g. Pushkarev et al., 2003; Bottema and van Vledder, 2008) and is usually discussed as an effect of wind input or as a

Nonlin. Processes Geophys. Discuss., doi:10.5194/npg-2016-61, 2016
Manuscript under review for journal Nonlin. Processes Geophys.
Published: 17 October 2016

Nonlinear Processes in Geophysics
Discussions
Open Access
EGU

transitional effect. Our simulations and the theoretical background of sect. 2.1 propose an alternative interpretation of the effect in terms of properties of general stationary solutions (7) for the kinetic equation (1). Fig. 7 shows clearly the presence of the second angular harmonics that can be predicted within the formal procedure of Pushkarev et al. (2003, 2004). Such treatment is not fully correct in the vicinity of the spectral peak but is still looks plausible. The second and higher harmonics of (7) are strongly decaying with frequency (e.g. Zakharov, 2010) and their accurate account requires special analysis. In the next section we present more evidences of their presence in the swell solutions.

3.4 Swell spectra vs KZ solutions

Very slow evolution of swell in our simulations provides a chance to check relevance of the classic Kolmogorov-Zakharov solutions (4-7) to the problem under study. The key feature of the swell solution from the theoretical viewpoint is its 'hybrid' (in words of Badulin et al., 2005) nature: inverse cascade determines evolution of wave spectral peak and its downshifting while the direct cascade occurs at frequencies slightly (approximately 20%) above the peak. This hybrid nature is illustrated by fig. 8 for energy and wave momentum fluxes. In order to avoid ambiguity in treatment of the simulation results within the weak turbulence theory we will not discuss this hybrid nature of swell solutions and focus on the direct cascade range. Thus, general solution (7) in the form

$$E(\omega,\theta) == \frac{P^{1/3}g^{4/3}}{\omega^4}G(0,gM/(\omega P),\theta)$$

and its approximate explicit version (6) by Katz and Kontorovich (1971) will be used below for describing the direct cascading of energy and momentum at high (as compared to ω_p) frequency.

Positive fluxes P and M decays with time in good agreement with power-law dependencies (20) and have rather low variations in relatively wide frequency range $3\omega_p < \omega < 7\omega_p$ in fig. 8. This domain of quasi-constant fluxes can be used for verification of results of the weak turbulence theory.

The first and the second Kolmogorov's constants can be easily estimated using the approximate solution (6) from combinations of along- and counter-propagating spectral densities as follows

$$C_p = \frac{\omega^4\,(E(\omega,0)+E(\omega,\pi))}{4g^{4/3}P^{1/3}} \tag{31}$$

$$C_m = \frac{\omega^5 P^{2/3}\,(E(\omega,0)-E(\omega,\pi))}{4g^{7/3}M}. \tag{32}$$

The corresponding values are shown in fig. 9. The found estimates of Kolmogorov's constants $C_p \approx 0.21 \pm 0.01$ and $C_m \approx 0.08 \pm 0.02$ are consistent with previous results (Lavrenov et al., 2002; Pushkarev et al., 2003; Badulin et al., 2005). Note, that the cited papers used different definitions of C_p, C_m. Here we follow ones of Zakharov (2010) (see eqs. 4-6).

Estimate of the second Kolmogorov constant C_m requires special comments as far as its correctness can be affected by higher-order terms (higher angular harmonics) of the solution (6). We see a possible effect of these corrections in relatively strong variations of estimates for the range $\omega/\omega_p < 4$ in fig. 9*b*. While the estimates of the Kolmogorov's constants for the swell look consistent the numerical solutions differ essentially from the approximate weakly anisotropic KZ solution (6). The

Nonlin. Processes Geophys. Discuss., doi:10.5194/npg-2016-61, 2016
Manuscript under review for journal Nonlin. Processes Geophys.
Published: 17 October 2016

angular spreading cannot be described by the only angular harmonics as in (6), higher-order corrections are clearly seen in figs.7 as side lobes. Nevertheless, the robustness of the estimates of the second Kolmogorov constant C_m provides a good benchmark for the balance of spectral fluxes and energy level in the wave spectra.

4 Discussion. Swell and ocean environment

Results of our simulations showed their fairly good correspondence to findings of the theory of wave (weak) turbulence. Relevance of these results to experimental facts seems to be a logical close of this work. The issue of relevance is two-fold. First, our results can help in explaining effects which interpretation in terms of alternative approaches (mostly, within linear theory) is questionable. Secondly, one can formulate, or, at least, sketch cases where our approach becomes invalid or requires an extension. Both aspects are considered in this section.

Attenuation in course of long term swell evolution is a burning problem of the swell monitoring. We show that contribution of wave-wave interactions to this process can be important mostly at initial stages of swell evolution. Thus, the observed rates of swell attenuation in an open ocean cannot be treated within our approach.

Ocean swell at long times (fetches) becomes likely an important constituent of the ocean environment as one heavily affected by relatively short wind-driven waves. We show that such interaction can lead to swell amplification at rather low wind speeds. This mechanism of swell transformation has not found adequate attention yet.

4.1 Swell attenuation within the kinetic equation

Dependence of wave height on time is shown in upper panel of fig. 10 for the 'almost isotropic' run `sw330`. Strong drop up to 30% of initial value occurs at relatively short time of about one day. Essential part of the wave energy leakage corresponds to this transitional stage at the very beginning of swell evolution when swell is tending very rapidly to self-similar asymptotics. Afterwards the decay becomes much slower following the power-law dependence for the self-similar solutions (20) fairly well.

For comparison with other models and available observations the duration-limited simulations have been recasted into dependencies on fetch through the simplest time-to-fetch transformation (e.g. Hwang and Wang, 2004; Hwang, 2006):

$$x(s) = \int_0^s C_g(\omega_p(t))dt. \tag{33}$$

The equivalent fetch is estimated as a distance covered by wave guide travelling with the group velocity of the spectral peak component. As seen in fig. 10 our model predicts an abrupt drop of wave height at distances shorter than 1000 km. In their turn, two quasi-linear models by Ardhuin et al. (2009) and Babanin (2006) predict gradual decay of swell up to 10% of initial wave height at distances 7000 km where our model shows qualitatively different weak attenuation.

It should be noted that our model describes attenuation of the ocean swell 'on its own' due to wave-wave interactions without any external effects. Thus, the effect of an abrupt drop of wave amplitude at short time (fetch) should be taken into consideration above all others when discussing possible application of our results to swell observations and physical interpretation of the experimental results.

Nonlin. Processes Geophys. Discuss., doi:10.5194/npg-2016-61, 2016
Manuscript under review for journal Nonlin. Processes Geophys.
Published: 17 October 2016

4.2 Swell and wind sea coupling. Arrest of weakly turbulent cascading

Extremely weak attenuation of swell due to wave-wave interactions provokes a question on robustness of this effect. A variety of physical effects in the ocean environment can change the swell evolution qualitatively. The above discussion of swell attenuation presents a remarkable example of such transformation when dissipative effects become dominant. Tracking of swell events from space gives an alternative scenario of transformation when swell appears to be growing. Satellite tracks can comprise up to 30% cases of growing swell 'most of them are not statistically significant' (Jiang et al., 2016). Nevertheless, a possible effect of wind sea background on long ocean swell opens an important discussion in view of theoretical (Badulin et al., 2008b) and experimental (Benilov et al., 1974; Badulin and Grigorieva, 2012) results that demonstrate swell amplification by wind wave background.

Simple estimates of the effect of relatively short wind-driven waves on long swell cam be made within the approach of wave turbulence. The idea of the estimates comes from the nature of the stationary Kolmogorov-Zakharov solutions where the spectral balance is supported by spectral fluxes. As noted in previous sections swell solution corresponds to the direct cascade of energy at frequencies approximately 20% higher than frequency of spectral peak. Energy is transferring from low to high frequencies by this mechanism. In their turn, growing wind waves are associated with inverse cascade that transfer energy in opposite direction from high to low frequencies and, thus, can arrest the direct cascade and force swell to grow. Thus, magnitudes of spectral fluxes associated with swell and with wind waves can give criteria of the flux arrest and possible amplification of swell by wind-driven waves. The spectral flux of direct cascade due to swell can be expressed in terms of the swell height (energy) and its peak frequency ω_p with the so-called weakly turbulent growth law (Badulin et al., 2007, eq.1.9). The same law accompanied by empirical dependencies of wind-wave growth can be used for estimating the magnitude of inverse cascade of wind waves (Gagnaire-Renou et al., 2011, Table 1). Skipping trivial algebra one can arrive at remarkably simple condition of balance of the fluxes written in terms of swell steepness μ_{swell} defined by (15) and inverse wave age of swell U_{10}/C_{swell} (C_{swell} being phase velocity of spectral peak component of swell and U_{10} is wind speed at a reference height)

$$2\frac{\rho_a}{\rho_w}\frac{U_{10}}{C_{swell}} \approx \mu_{swell}^2. \tag{34}$$

Small ratio of densities of air ρ and water ρ_w appears in (34) as a measure of weakness of the swell and wind sea coupling. The latter is not always true for mixed sea state where scales of wind waves and swell can be quite close. Moreover, even for well separated scales with frequency ratio two or more (wave length ratio 4 or more) the coupling of swell and wind-driven waves can be anomalously strong (see Badulin et al., 2008b). Anyway, the relationship (34) gives a ground for further studies of the effect.

In our simulations (e.g. Table1) steepness μ_{swell} varied in a wide range from initial $\mu \approx 0.15$ to final values below 0.01. Value $\mu = 0.01$ gives inverse wave age 0.04 in (34). For phase speed $C_{swell} = 25$ m$\cdot$s^{-1} (wave period $T_p \approx 16.2$s, wavelength $\lambda \approx 405$m) the corresponding wind speed appears quite low, approximately 1m$\cdot$s^{-1}.

Nonlin. Processes Geophys. Discuss., doi:10.5194/npg-2016-61, 2016
Manuscript under review for journal Nonlin. Processes Geophys.
Published: 17 October 2016

Thus, the simple estimate clearly shows a limited value of our 'pure swell' model for ocean environment. Potentially, the effect of even light wind on long-term propagation of swell can change result qualitatively. Our pilot numerical studies show importance of the swell and wind-sea coupling. This effect will be detailed in our further studies.

5 Conclusions

We presented results of sea swell simulations within the framework of the kinetic equation for water waves (the Hasselmann equation) and treated these properties within the paradigm of the theory of weak turbulence. A series of numerical experiments (duration-limited setup, WRT algorithm) has been carried out in order to outline features of wave spectra in a range of scales usually associated with ocean swell, i.e. wavelengths larger than 100 meters and duration of propagation up to 10^6 seconds (≈ 11.5 days). It should be stressed that the exact collision integral S_{nl} (nonlinear transfer term) has been used in all the calculations. Alternative, mostly operational approaches, like DIA (Discrete Approximation Approach) can corrupt the results qualitatively.

Fix the key results of the study

1. First, the classic Kolmogorov-Zakharov (KZ) isotropic and weakly anisotropic solutions for direct and inverse cascades are shown to be relevant to slowly evolving sea swell solutions. Estimates of the corresponding KZ constants are found to agree well with previous works. Thus, KZ solutions can be used as a benchmark for advanced approaches in the swell studies;

2. A strong tendency to self-similar asymptotics is demonstrated. These asymptotics are shown to be insensitive to initial conditions. In particular, universal angular distributions of wave spectra at large times have been obtained for both narrow (initial angular spreading $30°$) and almost isotropic initial spectra. The universality of the spectral shaping can be treated as an effect of mode selection when very few of eigenmodes of the boundary problem determines the system evolution. The inherent features of wave-wave interactions are responsible for this universality making the effect of initial conditions insignificant. Initial conditions can affect rates of the tendency to this asymptotic universal state. Generally, we observe the self-similar swell development in a background which is far from self-similar state;

3. We show that an inherent peculiarity of the Hasselmann equation, energy leakage, can also be considered as a mechanism of the sea swell attenuation. This mechanism is not accounted for by the today models of sea swell. In the meantime, the energy decay rates of sea swell in the numerical experiments, generally, do not contradict to results of swell observations. These observations are focused mostly on 'far field' behavior of swell, generally, 1000 or more kilometers away from a stormy area. Our simulations show that dramatic transformation of the swell due to wave-wave interactions occurs at shorter distances, in 'near field'. Thus, fig.10 illustrates different domains of model relevance rather than applicability of the different models for studies of ocean swell;

4. Long term evolution of swell is associated with rather slow frequency downshift ($\omega_p \sim t^{-1/11}$) and energy attenuation ($E \sim t^{-1/11}$). Meanwhile, the decay of other wave field quantities is essentially faster: wave steepness is decaying as

Nonlin. Processes Geophys. Discuss., doi:10.5194/npg-2016-61, 2016
Manuscript under review for journal Nonlin. Processes Geophys.
Published: 17 October 2016

$\mu \sim t^{-5/22}$ and total spectral flux even faster $dE/dt \sim t^{-12/11}$. This point is of key importance in our analysis as far as we consider nonlinear cascades of wave energy as governing physical mechanism of swell evolution. As we showed in Discussion at sufficiently long times the weak direct cascade of swell can be arrested by quite light wind and then swell can start to grow. Satellite data (Jiang et al., 2016) and analysis of visual observations (Badulin and Grigorieva, 2012), in our opinion, provide telling arguments for this effect. Thus, 'negative dissipation' of swell (in words of Jiang et al., 2016) could find its explanation within the simple estimate of sect.4.2;

5. The last conclusion uncovers deficiency of the duration-limited setup for the phenomenon of swell. An alternative setup of fetch-limited evolution ($\partial/\partial t \equiv 0$, $\nabla_{\mathbf{r}} \neq 0$) introduces dispersion of wave harmonics as a competing mechanism that can change the swell evolution dramatically. Recent advances in wave modelling (Pushkarev and Zakharov, 2016) makes the problem of spatial-temporal swell evolution feasible and specify the direction of our further work. The present paper can be considered as the very first step.

Acknowledgements. Authors are thankful for the support of the Russian Science Foundation grant No. 14-22-00174. Authors are indebted to Prof. Victor Shrira and Vladimir Geogjaev for discussions and valuable comments.

Nonlin. Processes Geophys. Discuss., doi:10.5194/npg-2016-61, 2016
Manuscript under review for journal Nonlin. Processes Geophys.
Published: 17 October 2016

References

Ardhuin, F., Chapron, B., and Collard, F.: Observation of swell dissipation across oceans, Geophys. Res. Lett., 36, L06607, doi:10.1029/2008GL037030, 2009.

Ardhuin, F., Rogers, E., Babanin, A. V., Filipot, J.-F., Magne, R., Roland, A., van der Westhuysen, A., Queffeulou, P., Aouf, J.-M. L. L., and Collard, F.: Semiempirical Dissipation Source Functions for Ocean Waves. Part I: Definition, Calibration, and Validation, J. Phys. Oceanogr., 40, 1917–1941, doi:10.1175/2010JPO4324.1, 2010.

Babanin, A. V.: On a wave-induced turbulence and a wave mixed upper ocean layer, Geophys. Res. Lett., 33, L20 605, doi:10.1029/2006GL027308, 2006.

Badulin, S. I. and Grigorieva, V. G.: On discriminating swell and wind-driven seas in Voluntary Observing Ship data, J. Geophys. Res., 117, doi:10.1029/2012JC007937, 2012.

Badulin, S. I., Pushkarev, A. N., Resio, D., and Zakharov, V. E.: Direct and inverse cascade of energy, momentum and wave action in wind-driven sea, in: 7th International workshop on wave hindcasting and forecasting, pp. 92–103, Banff, October 2002, 2002.

Badulin, S. I., Pushkarev, A. N., Resio, D., and Zakharov, V. E.: Self-similarity of wind-driven seas, Nonl. Proc. Geophys., 12, 891–946, 2005.

Badulin, S. I., Babanin, A. V., Resio, D., and Zakharov, V.: Weakly turbulent laws of wind-wave growth, J. Fluid Mech., 591, 339–378, 2007.

Badulin, S. I., Babanin, A. V., Resio, D., and Zakharov, V.: Numerical verification of weakly turbulent law of wind wave growth, in: IUTAM Symposium on Hamiltonian Dynamics, Vortex Structures, Turbulence. Proceedings of the IUTAM Symposium held in Moscow, 25-30 August, 2006, edited by Borisov, A. V., Kozlov, V. V., Mamaev, I. S., and Sokolovskiy, M. A., vol. 6 of *IUTAM Bookseries*, pp. 175–190, Springer, ISBN: 978-1-4020-6743-3, 2008a.

Badulin, S. I., Korotkevich, A. O., Resio, D., and Zakharov, V. E.: Wave-wave interactions in wind-driven mixed seas, in: Proceedings of the Rogue waves 2008 Workshop, pp. 77–85, IFREMER, Brest, France, 2008b.

Balk, A. M.: On the Kolmogorov-Zakharov spectra of weak turbulence, Phys. D: Nonlin. Phenom., 139, 137–157, 2000.

Barrenblatt, G. I.: Scaling, self-similarity, and intermediate asymptotics : Dimensional analysis and intermediate asymptotics, Plenum Press, New York/London, 1979.

Benilov, A. Y., Kouznetsov, O. A., and Panin, G. N.: On the analysis of wind wave-induced disturbances in the atmospheric turbulent surface layer, Boundary-Layer Meteorol., 6, 269–285, 1974.

Benoit, M. and Gagnaire-Renou, E.: Interactions vague-vague non-linéaires et spectre d'équilibre pour les vagues de gravité en grande profondeur d'eau, in: Proc. 18th Congrès Français de Mécanique, Grenoble (France), 2007.

Bottema, M. and van Vledder, G. P.: Effective fetch and non-linear four-wave interactions during wave growth in slanting fetch conditions, Coastal Eng., 55, 261–275, 2008.

Bottema, M. and van Vledder, G. P.: A ten-year data set for fetch- and depth-limited wave growth, Coastal Eng., 56, 703–725, 2009.

Chen, K. S., Chapron, B., and Ezraty, R.: A Global View of Swell and Wind Sea Climate in the Ocean by Satellite Altimeter and Scatterometer, J. Phys. Oceanogr., 19, 2002.

Donelan, M. A., Hamilton, J., and Hui, W. H.: Directional spectra of wind-generated waves, Phil. Trans. Roy. Soc. Lond. A, 315, 509–562, 1985.

Gagnaire-Renou, E., Benoit, M., and Forget, P.: Ocean wave spectrum properties as derived from quasi-exact computations of nonlinear wave-wave interactions, J. Geophys. Res., 2010.

Gagnaire-Renou, E., Benoit, M., and Badulin, S. I.: On weakly turbulent scaling of wind sea in simulations of fetch-limited growth, J. Fluid Mech., 669, 178–213, 2011.

Hasselmann, K.: On the nonlinear energy transfer in a gravity wave spectrum. Part 1. General theory, J. Fluid Mech., 12, 481–500, 1962.

Hasselmann, K., Ross, D. B., Müller, P., and Sell, W.: A parametric wave prediction model, J. Phys. Oceanogr., 6, 200–228, 1976.

Hasselmann, S. and Hasselmann, K.: Computations and parametrizations of the nonlinear energy transfer in a gravity-wave spectrum. Part I. A new method for efficient computations of the exact nonlinear transfer integral, J. Phys. Oceanogr., 15, 1369–1377, 1985.

Henderson, D. M. and Segur, H.: The role of dissipation in the evolution of ocean swell, J. Geophys. Res. Oceans, 118, 5074–5091, doi:10.1002/jgrc.20324, 2013.

Hwang, P. A.: Duration and fetch-limited growth functions of wind-generated waves parameterized with three different scaling wind velocities, J. Geophys. Res., 111, doi:10.1029/2005JC003 180, 2006.

Hwang, P. A. and Wang, D. W.: Field measurements of duration-limited growth of wind-generated ocean surface waves at young stage of development, J. Phys. Oceanogr., 34, 2316–2326, 2004.

Jiang, H., Stopa, J. E., Wang, H., Husson, R., Mouche, A., Chapron, B., and Chen, G.: Tracking the attenuation and nonbreaking dissipation of swells using altimeters, J. Geophys. Res. Oceans, doi:10.1002/2015JC011536, 2016.

Katz, A. V. and Kontorovich, V. M.: Drift stationary solutions in the weak turbulence theory, JETP Letters, 14, 265–267, 1971.

Katz, A. V. and Kontorovich, V. M.: Anisotropic turbulent distributions for waves with a non-decay dispersion law, Soviet Physics JETP, 38, 102–107, 1974.

Komen, G. J., Hasselmann, S., and Hasselmann, K.: On the existence of a fully developed wind-sea spectrum, J. Phys. Oceanogr., 14, 1271–1285, 1984.

Lavrenov, I., Resio, D., and Zakharov, V.: Numerical simulation of weak turbulent Kolmogorov spectrum in water surface waves, in: 7th International workshop on wave hindcasting and forecasting, pp. 104–116, Banff, October 2002, 2002.

Munk, W. H., Miller, G. R., Snodgrass, F. E., and Barber, N. F.: Directional Recording of Swell from Distant Storms, Phil. Trans. Roy. Soc. London, 255, 505–584, 1963.

Pettersson, H.: Wave growth in a narrow bay, Ph.D. thesis, University of Helsinki, http://ethesis.helsinki.fi/julkaisut/mat/fysik/vk/pettersson/, [ISBN 951-53-2589-7 (Paperback) ISBN 952-10-1767-8 (PDF)], 2004.

Phillips, O. M.: On the dynamics of unsteady gravity waves of finite amplitude, J. Fluid Mech., 9, 193–217, 1960.

Pushkarev, A. and Zakharov, V.: On nonlinearity implications and wind forcing in Hasselmann equation, ArXiv e-prints, 2015.

Pushkarev, A. and Zakharov, V.: Limited fetch revisited: Comparison of wind input terms, in surface wave modeling, Ocean Modelling, pp. –, doi:http://dx.doi.org/10.1016/j.ocemod.2016.03.005, http://www.sciencedirect.com/science/article/pii/S1463500316300026, 2016.

Pushkarev, A. N., Resio, D., and Zakharov, V. E.: Weak turbulent theory of the wind-generated gravity sea waves, Phys. D: Nonlin. Phenom., 184, 29–63, 2003.

Pushkarev, A. N., Resio, D., and Zakharov, V. E.: Second generation diffusion model of interacting gravity waves on the surface of deep water, Nonl. Proc. Geophys., 11, 329–342, sRef-ID: 1607-7946/npg/2004-11-329, 2004.

Snodgrass, F. E., Groves, G. W., Hasselmann, K. F., Miller, G. R., Munk, W. H., and Powers, W. H.: Propagation of Ocean Swell across the Pacific, Phil. Trans. Roy. Soc. London, 259, 431–497, 1966.

Tracy, B. and Resio, D.: Theory and calculation of the nonlinear energy transfer between sea waves in deep water, WES Rep. 11, US Army, Engineer Waterways Experiment Station, Vicksburg, MS, 1982.

Webb, D. J.: Non-linear transfers between sea waves, Deep Sea Res., 25, 279–298, 1978.

Young, I. R.: Directional spectra of hurricane wind waves, J. Geophys. Res., 111, doi:10.1029/2006JC003 540, 2006.

Young, I. R., Babanin, A. V., and Zieger, S.: The Decay Rate of Ocean Swell Observed by Altimeter, J. Phys. Oceanogr., 43, 2322–2333, 2013.

Zakharov, V. E.: Statistical theory of gravity and capillary waves on the surface of a finite-depth fluid, Eur. J. Mech. B/Fluids, 18, 327–344, 1999.

Zakharov, V. E.: Theoretical interpretation of fetch limited wind-driven sea observations, Nonl. Proc. Geophys., 12, 1011–1020, 2005.

Zakharov, V. E.: Energy balance in a wind-driven sea, Phys. Scr., T142, 014 052, doi:10.1088/0031-8949/2010/T142/014052, 2010.

Zakharov, V. E. and Badulin, S. I.: On Energy Balance in Wind-Driven Seas, Doklady Earth Sciences, 440, 1440–1444, 2011.

Zakharov, V. E. and Filonenko, N. N.: Energy spectrum for stochastic oscillations of the surface of a fluid, Soviet Phys. Dokl., 160, 1292–1295, 1966.

Zakharov, V. E. and Pushkarev, A. N.: Diffusion model of interacting gravity waves on the surface of deep fluid, Nonl. Proc. Geophys., 6, 1–10, 1999.

Zakharov, V. E. and Zaslavsky, M. M.: Kinetic equation and Kolmogorov spectra in the weak-turbulence theory of wind waves, Izv. Atmos. Ocean. Phys., 18, 970–980, 1982.

Zakharov, V. E., Lvov, V. S., and Falkovich, G.: Kolmogorov spectra of turbulence. Part I, Springer, Berlin, 1992.

Zakharov, V. E., Badulin, S. I., Hwang, P. A., and Caulliez, G.: Universality of Sea Wave Growth and Its Physical Roots, J. Fluid Mech., 708, 503–535, doi:10.1017/jfm.2015.468, 2015.

Zaslavskii, M. M.: Nonlinear evolution of the spectrum of swell, Izv. Atmos. Ocean. Phys., 36, 253–260, 2000.

Nonlin. Processes Geophys. Discuss., doi:10.5194/npg-2016-61, 2016
Manuscript under review for journal Nonlin. Processes Geophys.
Published: 17 October 2016

Nonlinear Processes in Geophysics
Discussions
Open Access
EGU

Table 1. Initial parameters of simulation series

ID	Θ	N (m$^2 \cdot s$)	H_s (m)
sw030	30°	0.720	4.63
sw050	60°	0.719	4.6
sw170	180°	0.714	4.74
sw230	240°	0.721	4.67
sw330	330°	0.722	4.79

Nonlin. Processes Geophys. Discuss., doi:10.5194/npg-2016-61, 2016
Manuscript under review for journal Nonlin. Processes Geophys.
Published: 17 October 2016

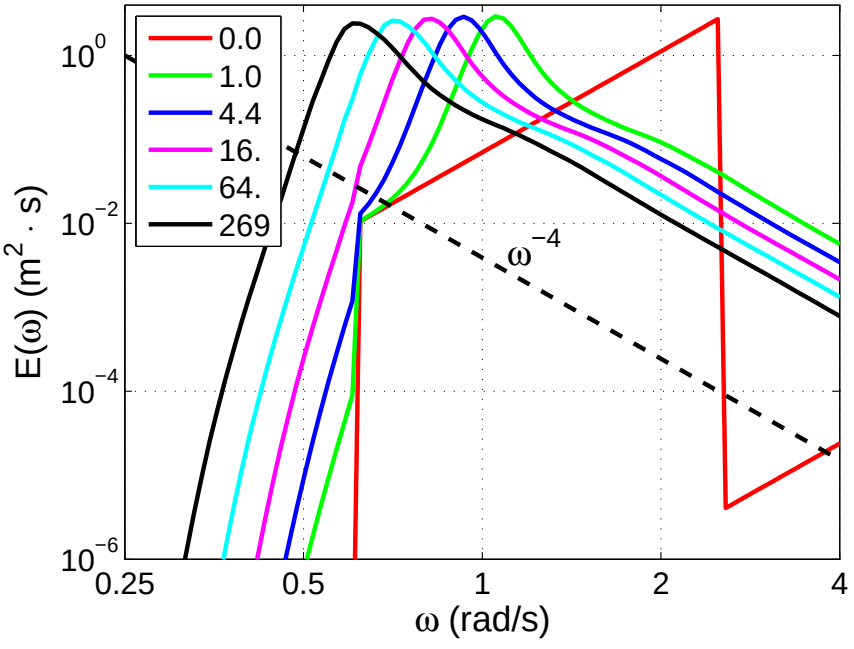

Figure 1. Frequency spectra at different times (legend, in hours) for the case sw330 ($\Theta = 330°$).

Nonlin. Processes Geophys. Discuss., doi:10.5194/npg-2016-61, 2016
Manuscript under review for journal Nonlin. Processes Geophys.
Published: 17 October 2016

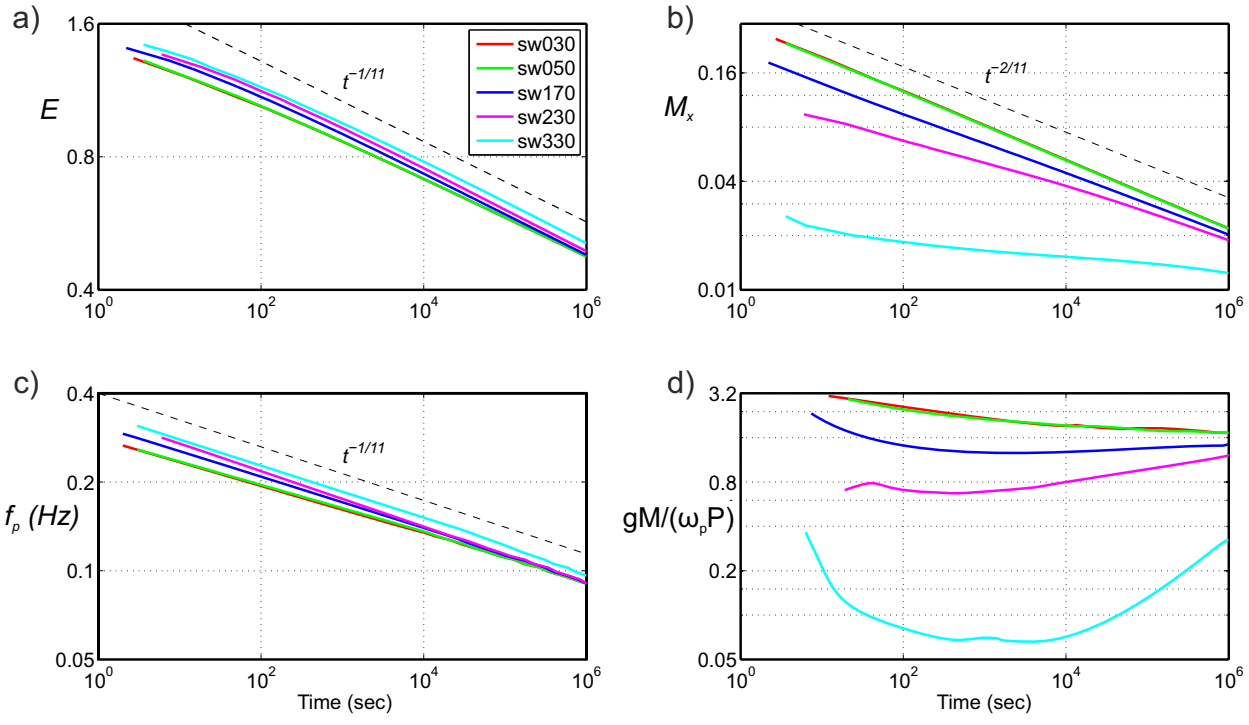

Figure 2. Evolution of wave parameters for runs of Table 1 (in legend): *a)* – total energy E; *b)* -total wave momentum M; *c)* – frequency $f_p = \omega_p/(2\pi)$ of the energy spectra peak; *d)* – estimate of parameter of anisotropy in the Kolmogorov-Zakharov solution (6). Dashed lines show asymptotic power laws (20,22)

Nonlin. Processes Geophys. Discuss., doi:10.5194/npg-2016-61, 2016
Manuscript under review for journal Nonlin. Processes Geophys.
Published: 17 October 2016

Nonlinear Processes in Geophysics
Discussions
Open Access
EGU

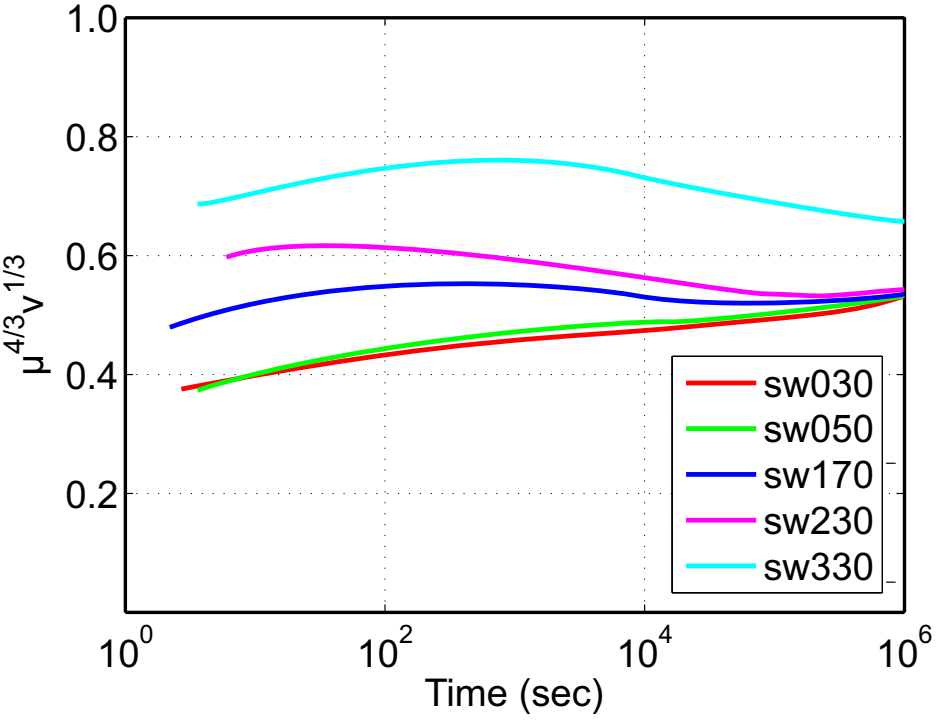

Figure 3. Evolution of the left-hand side of the invariant (14) $(\mu^4\nu)^{1/3}$ for runs of Table 1 (in legend).

Nonlin. Processes Geophys. Discuss., doi:10.5194/npg-2016-61, 2016
Manuscript under review for journal Nonlin. Processes Geophys.
Published: 17 October 2016

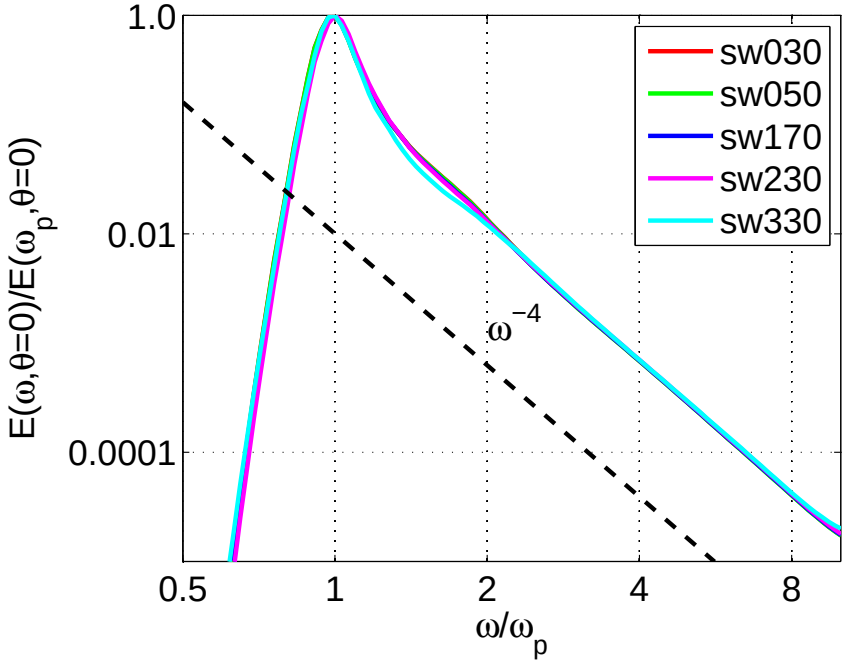

Figure 4. Normalized frequency spectra for direction $\theta = 0°$ after 11.5 days (approximately 10^6 seconds) of swell evolution for runs of Table 1 (see legend).

Nonlin. Processes Geophys. Discuss., doi:10.5194/npg-2016-61, 2016
Manuscript under review for journal Nonlin. Processes Geophys.
Published: 17 October 2016

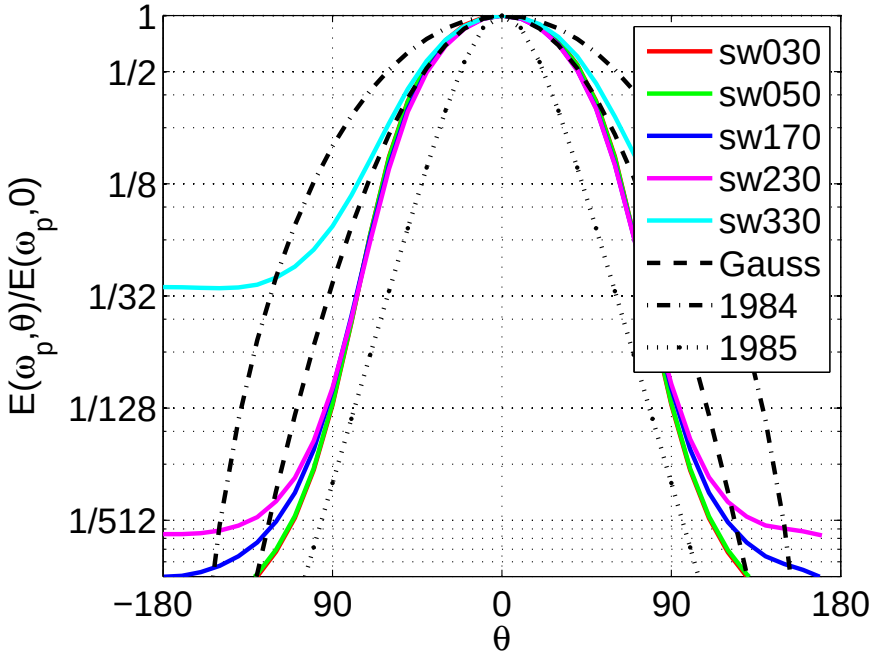

Figure 5. Normalized dependence of swell energy spectra on angle at peak frequency ω_p after 11.5 days (approximately 10^6 seconds) of swell evolution for runs of Table 1 (see legend). Dashed line – Gaussian distribution (28) with dispersion $\sigma_\Theta = 35°$; dash-dot – fully developed sea (30) and eq.3.6-3.7 of Komen et al. (1984); dotted – growing sea (29) and eq.9.1-9.2 of Donelan et al. (1985).

Nonlin. Processes Geophys. Discuss., doi:10.5194/npg-2016-61, 2016
Manuscript under review for journal Nonlin. Processes Geophys.
Published: 17 October 2016

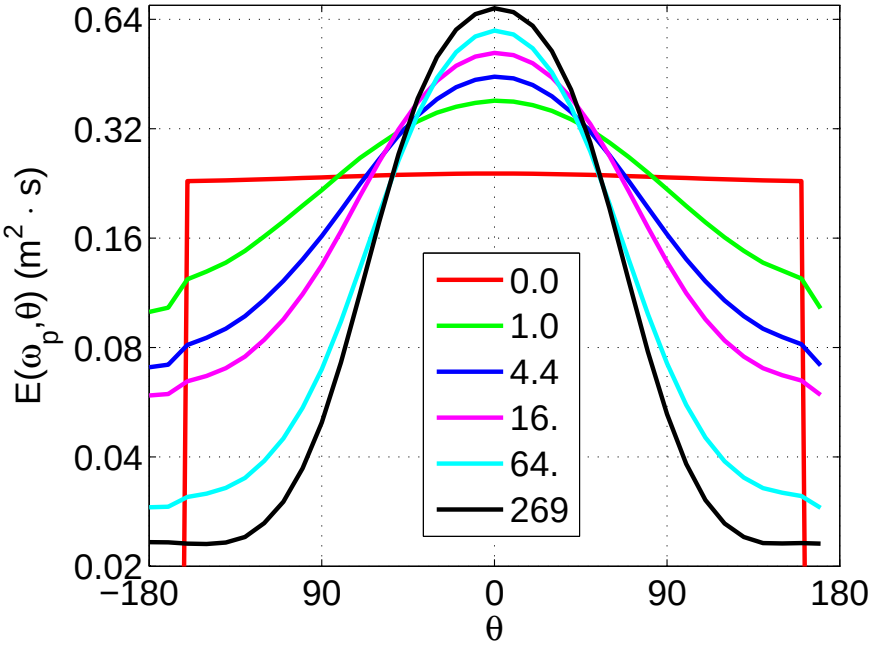

Figure 6. Angular distributions at the spectra peak frequency at different times (legend, in hours) for the case `sw330`.

Nonlin. Processes Geophys. Discuss., doi:10.5194/npg-2016-61, 2016
Manuscript under review for journal Nonlin. Processes Geophys.
Published: 17 October 2016

Nonlinear Processes in Geophysics
Discussions
Open Access
EGU

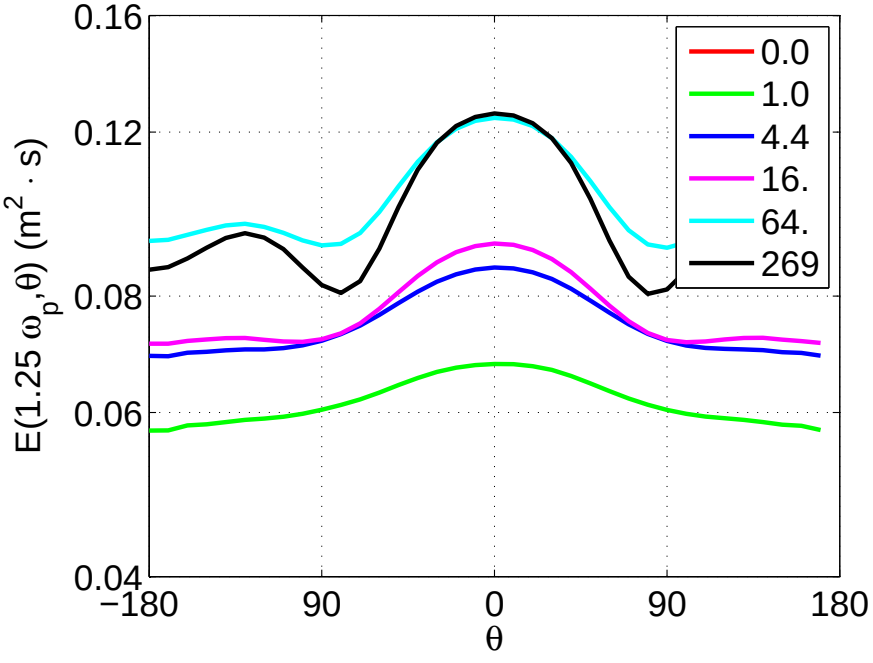

Figure 7. Angular distributions at frequency $1.25\omega_p$ at different times (legend, in hours) for the case `sw330`. Spectrum at $t = 0$ is beyond of y-axis lower limit.

Nonlin. Processes Geophys. Discuss., doi:10.5194/npg-2016-61, 2016
Manuscript under review for journal Nonlin. Processes Geophys.
Published: 17 October 2016

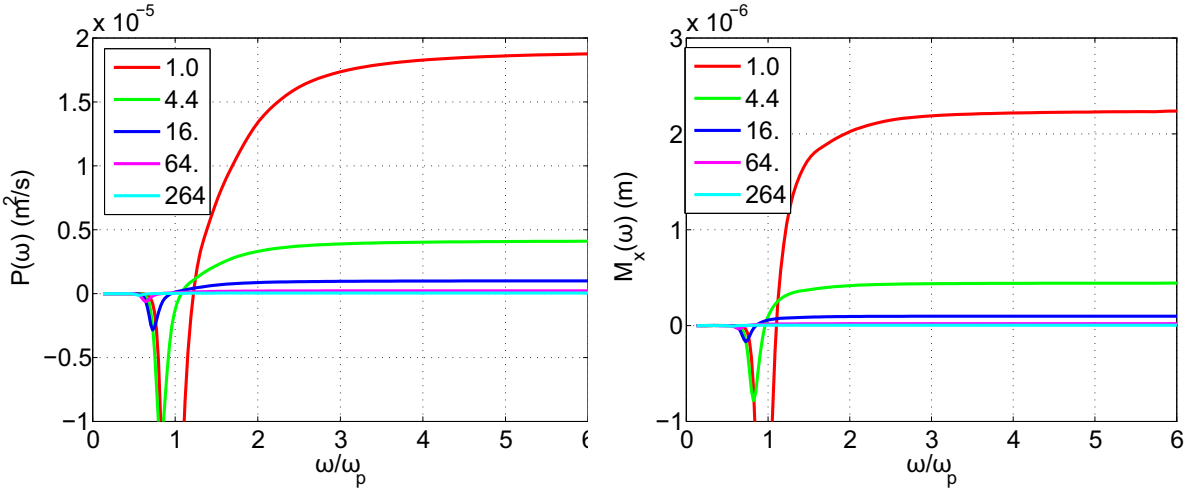

Figure 8. Left – spectral fluxes of energy, right – of the $x-$ component of wave momentum M_x at different times (legend, in hours) for the case sw170.

Nonlin. Processes Geophys. Discuss., doi:10.5194/npg-2016-61, 2016
Manuscript under review for journal Nonlin. Processes Geophys.
Published: 17 October 2016

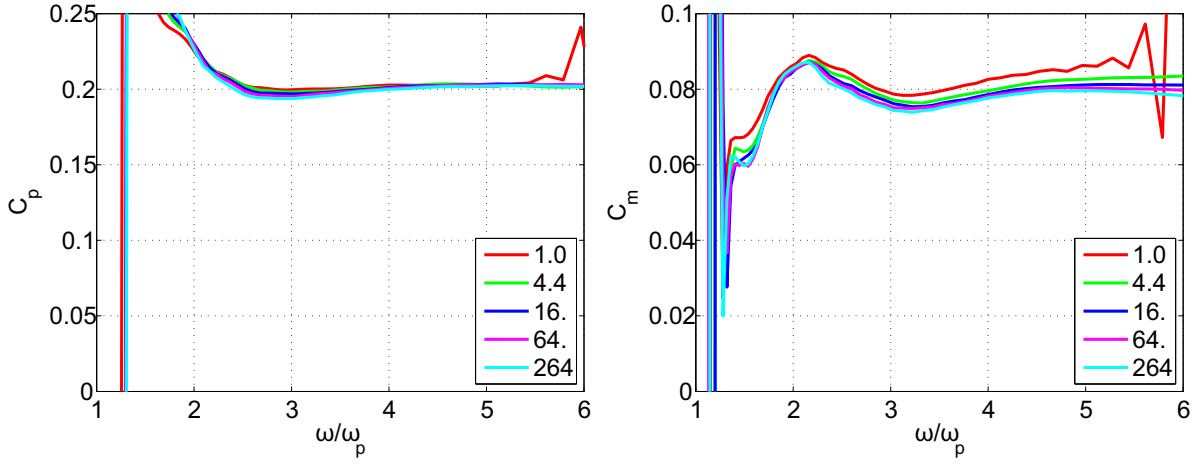

Figure 9. Left – estimate of the first Kolmogorov constant C_p, right – estimate of the second Kolmogorov constant C_m for the approximate anisotropic KZ solution (6). Time in hours is given in legend for the case sw170.

Nonlin. Processes Geophys. Discuss., doi:10.5194/npg-2016-61, 2016
Manuscript under review for journal Nonlin. Processes Geophys.
Published: 17 October 2016

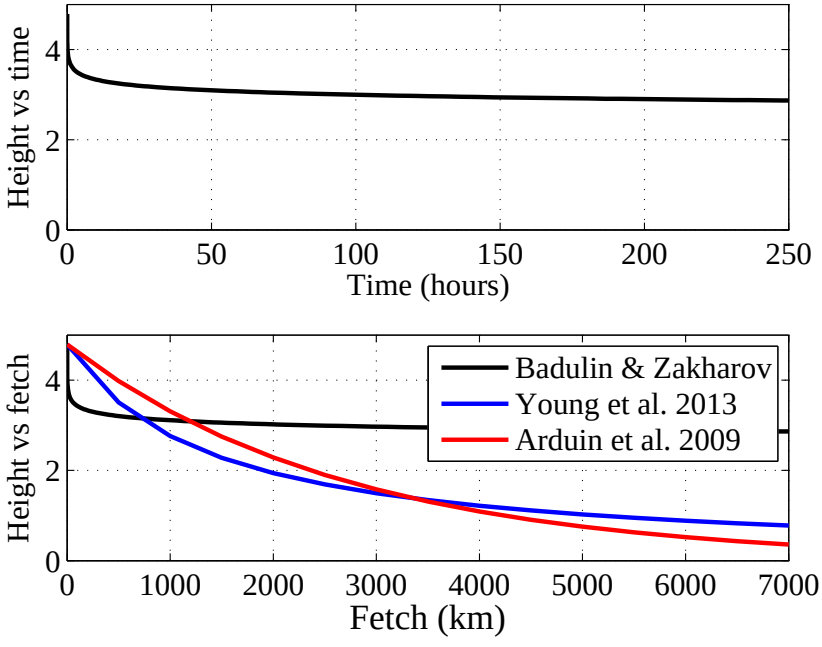

Figure 10. Top – dependence of significant wave height H_s on time for the case `sw330`. Bottom – attenuation of swell for models Ardhuin et al. (2009); Young et al. (2013) and one of this paper (see ledend). Results of duration-limited simulations are recasted into dependencies on fetch by simple transformation (33).